

The first chemical enrichment in the universe and the formation of hyper metal-poor stars

Nobuyuki Iwamoto,¹ Hideyuki Umeda,² Nozomu Tominaga,²
Ken'ichi Nomoto,^{2*} Keiichi Maeda³

¹Nuclear Data Center, Japan Atomic Energy Research Institute, Ibaraki 319-1195, Japan,

²Department of Astronomy, School of Science, University of Tokyo,
Tokyo 113-0033, Japan,

³Department of Earth Science and Astronomy, College of Arts and Sciences,
University of Tokyo, Tokyo 153-8902, Japan

*To whom correspondence should be addressed; E-mail: nomoto@astron.s.u-tokyo.ac.jp.

**To be published in Science, and within the Science Express web site
(<http://www.scienceexpress.org>) on 2 June 2005**

The recent discovery of a hyper metal-poor (HMP) star, whose metallicity Fe/H is smaller than 1/100,000 of the solar ratio, together with one earlier HMP star, has raised a challenging question if these HMP stars are the actual first generation, low mass stars in the Universe. We argue that these HMP stars are the second generation stars being formed from gases which were chemically enriched by the first generation supernovae. The key to this solution is the very unusual abundance patterns of these HMP stars with important similarities and differences. We can reproduce these abundance features with the core-collapse “faint” supernova models which un-

dergo extensive matter mixing and fallback during the explosion.

Identifying the first stars in the Universe, i.e., metal-free, Population III (Pop III) stars which were born in a primordial hydrogen-helium gas cloud is one of the important challenges of the current astronomy (1, 2). Recently two hyper metal-poor (HMP) stars, HE0107–5240 (3) and HE1327–2326 (4), were discovered, whose metallicity Fe/H is smaller than 1/100,000 of the Sun (i.e., $[\text{Fe}/\text{H}] < -5$), being more than a factor of 10 smaller than previously known extremely metal-poor (EMP) stars. (Here $[A/B] = \log_{10}(N_A/N_B) - \log_{10}(N_A/N_B)_\odot$, where the subscript \odot refers to the solar value and N_A and N_B are the abundances of elements A and B, respectively.) This discovery was raised an important question as to whether the observed low mass ($\sim 0.8 M_\odot$) HMP stars are actually Pop III stars, or whether these HMP stars are the second generation stars being formed from gases which were chemically enriched by a single first generation supernova (SN) (5). This is related to the questions of how the initial mass function depends on the metallicity (6). Thus identifying the origin of these HMP stars is indispensable to the understanding of the earliest star formation and chemical enrichment history of the Universe.

The elemental abundance patterns of these HMP stars provide a key to the answer to the above questions. The abundance patterns of HE1327–2326 (4) and HE0107–5240 (7, 8) are quite unusual (Fig. 1). The striking similarity of $[\text{Fe}/\text{H}]$ ($= -5.4$ and -5.2 for HE1327–2326 and HE0107–5240, respectively) and $[\text{C}/\text{Fe}]$ ($\sim +4$) suggests that similar chemical enrichment mechanisms operated in forming these HMP stars. However, the N/C and (Na, Mg, Al)/Fe ratios are more than a factor of 10 larger in HE1327–2326. In order for the theoretical models to be viable, these similarities and differences should be explained self-consistently.

Here we report our findings that the above similarities and variations of the HMP stars

can be well reproduced in unified manner by nucleosynthesis in the core-collapse “faint” supernovae (SNe) which undergo mixing-and-fallback (5). We thus argue that the HMP stars are the second generation low mass stars, whose formation was induced by the first generation (Pop III) SN with efficient cooling of carbon-enriched gases.

The similarity of $[\text{Fe}/\text{H}]$ and $[\text{C}/\text{Fe}]$ suggests that the progenitor’s masses of Pop III SNe were similar for these HMP stars. We therefore choose the Pop III $25 M_{\odot}$ models and calculate their evolution and explosion. The abundance distribution after explosive nucleosynthesis is shown in Figure 2 for the kinetic energy E of the ejecta $E_{51} \equiv E/10^{51} \text{ erg} = 0.74$. The abundance distribution for $E_{51} = 0.71$ is similar. In the “faint” SN model, most part of materials that underwent explosive nucleosynthesis are decelerated by the influence of the gravitational pull (9) and will eventually fall back onto the central compact object (Fig. 3). Such “fallback” was not calculated in ref. (5), but is found to take place in the present modeling if $E_{51} < 0.71$. (For the $50 M_{\odot}$ star, the fallback is found to occur for $E_{51} < 2$ because of deeper gravitational potential.) We obtain a relation between E and the mass cut M_{cut} (the mass of the materials which finally collapse to form a compact object), i.e., smaller E_{51} leads to a larger amount of fallback (larger M_{cut}). The explosion energies of $E_{51} = 0.74$ and 0.71 lead to the mass cut $M_{\text{cut}} = 5.8M_{\odot}$ and $6.3M_{\odot}$, respectively, and we use the former and the latter models to explain the abundance patterns of HE1327–2326 and HE0107–5240, respectively.

During the explosion, we assume that the SN ejecta undergoes mixing, i.e., materials are first uniformly mixed in the mixing-region extending from $M_r = 1.9M_{\odot}$ to the mass cut at $M_r = M_{\text{cut}}$ (where M_r is the mass coordinate and stands for the mass interior to the radius r) as indicated in Figure 2 (also see legend), and only a tiny fraction, f , of the mixed material is ejected from the mixing-region together with all materials at $M_r > M_{\text{cut}}$; most materials interior to the mass cut fall back onto the central compact

object. Such a mixing-fallback mechanism (which might mimic a jet-like explosion) is required to extract Fe-peak and other heavy elements from the deep fallback region into the ejecta (5, 10).

Figure 1 shows the calculated abundance ratios in the SN ejecta models for suitable choice of f (see legend of Fig. 2) which are respectively compared with the observed abundances of the two HMP stars. To reproduce $[\text{C}/\text{Fe}] \sim +4$ and other abundance ratios of HMP stars in Figure 1, the ejected mass of Fe is only $1.0 \times 10^{-5} M_{\odot}$ for HE1327–2326 and $1.4 \times 10^{-5} M_{\odot}$ for HE0107–5240 (see legend of Fig. 2 for other abundances). These SNe are much fainter in the radioactive tail than the typical SNe and form massive black holes of $\sim 6 M_{\odot}$.

The question is what causes the large difference in the amount of Na-Mg-Al between the SNe that produced HE0107–5240 and HE1327–2326. Because very little Na-Mg-Al is ejected from the mixed fallback materials (i.e., $f \sim 10^{-4}$) compared with the materials exterior to the mass cut, the ejected amount of Na-Mg-Al is very sensitive to the location of the mass cut. As indicated in Figure 2, M_{cut} is smaller (i.e., the fallback mass is smaller) in the model for HE1327–2326 ($M_{\text{cut}} = 5.8 M_{\odot}$) than HE0107–5240 ($M_{\text{cut}} = 6.3 M_{\odot}$), so that a larger amount of Na-Mg-Al is ejected from the SN for HE1327–2326. Since M_{cut} is sensitively determined by the explosion energy, the (Na-Mg-Al)/Fe ratios among the HMP stars are predicted to show significant variations and can be used to constrain E_{51} . Note also that the explosion energies of these SN models with fallback are not necessarily very small (i.e., $E_{51} \sim 0.7$). Further these explosion energies are consistent with those observed in the actual "faint" SNe (11).

Here we should note that our previous models (5) tend to underproduce Na compared with the abundances of HE0107–5240. This problem has been improved in our new presupernova models. Na and Al are mainly produced by C shell-burning, and their

production is very sensitive to the treatment of overshooting in the convective C burning shell as well as the ^{12}C abundance left after core He burning (12). By including overshooting with the overshooting length less than one-fifth of a pressure scale height for whole presupernova evolution, our new supernova models contain large enough abundances of Na and Al as seen in Figure 2. Such an overshooting length has been estimated from the comparison with the HR diagrams of many young stellar clusters. After the mixing-and-fallback, the resultant abundance patterns with Na and Al are in reasonable agreement with HE1327–2326 and HE0107–5240 (Fig. 1). The enhancement of Na and Al attributable to overshooting in the progenitor evolution may better explain the small odd-even effect in the elemental abundance patterns observed in EMP stars (13).

The next question is why HE1327–2326 has a much larger N/C ratio than HE0107–5240. In our models, a significant amount of N is produced by the mixing between the He convective shell and the H-rich envelope during the presupernova evolution (14), where C created by the triple- α reaction is burnt into N through the CNO cycle. For the HE1327–2326 model, we assume about 30 times larger diffusion coefficients (i.e., faster mixing) for the H and He convective shells to overcome an inhibiting effect of the mean molecular weight gradient (and also entropy gradient) between H and He layers. Thus, larger amounts of protons are carried into the He convective shell. Then $[\text{C}/\text{N}] \sim 0$ is realized as observed in HE1327–2326. Such an enhancement of mixing efficiency has been suggested to take place in the present-day massive stars known as fast rotators, which show various N and He enrichments due to different rotation velocities (15).

If no large enhancement of N occurred in the SN ejecta, the following scenario can explain high abundance of N (and also Na and Al) at the surface. If HE1327–2326 is in a binary system and its companion star had experienced the asymptotic giant branch (AGB) phase, only the odd-elements such as N, Na and Al can be efficiently enriched.

The observed C, Mg and heavier elements should predominantly come from a faint SN as modeled above. The small accreted mass (e.g., $\sim 10^{-4} - 10^{-3} M_{\odot}$) mixed with shallow surface convective layer in HE1327–2326 is enough to account for the observed abundance pattern. The smallness of the accreted mass requires that the observed star belongs to a wide binary system and accretion takes place through mass loss from an AGB star. In contrast to the AGB-scenario without the pre-enrichment from the faint SN (see below), this model can realize $[C/N] \sim 0$ if the proper amount of N is transferred.

For HE0107–5240, an alternative scenario has been proposed, assuming that the HMP stars are actually Pop III stars. Here we point out that such a scenario has difficulty in explaining the differences between HE0107–5240 and HE1327–2326. This scenario assumes that the HMP star is in a binary system and an AGB companion star has polluted the surface abundance of the HMP star (16). Even if Pop III AGB stars suffer any surface pollution at the early phase of their evolution (16, 17, 18), recurrent mixing-process after He shell flashes (third dredge-up) carries C-enriched materials (with no enrichment of N) from a deep He-rich layer to the surface. The surface C abundance of the low-mass companion progressively increases, but no N enhancement can be seen (i.e., $[C/N] > 0$). On the contrary, if a donor AGB star experiences hot bottom burning, dredged-up C is processed into N at the base of the convective envelope and thus $[C/N] = -2 \sim -1$. Therefore $[C/N] \approx 0$ is difficult to be reproduced by Pop III AGB stars, although the C/N ratio might be consistent with the observed value during a short period of the evolution.

What about stars with 130-300 M_{\odot} (19, 20)? Pair-instability SNe (PISNe) from this mass range have been widely considered to be the first source of chemical enrichment in the universe (20). However, PISNe provide abundance patterns that are incompatible with the observations of the HMP stars. Since PISNe undergo complete disruption and eject a large amount of Fe (19, 20), the ejecta have $[C/Fe]$ that is too low (< 0) to be

compatible with the two HMP stars and large $[\text{Fe}/\text{H}]$ (say > -4) is predicted.

What other elements are important to distinguish the different models? Oxygen is certainly important. For HE0107–5240, its large $[\text{C}/\text{O}]$ ratio rules out the simple mass-cut models (without mixing-fallback) in the multiple SN model (8, 10). For our faint SN models, $[\text{C}/\text{O}]$ is sensitive to M_{cut} and thus E .

Neutron-capture elements are important for constraining scenarios involving an AGB star. For HE1327–2326, the observed lower limit of $[\text{Sr}/\text{Ba}] > -0.4$ is inconsistent with the s-process enhanced stars (21, 22) and theoretical predictions of low metallicity AGB s-process (23), but is remarkably consistent with the values seen in the r-process enhanced stars (24, 25). This may favor SN origins because the r-process signature observed in EMP stars is thought to come from SNe, but one should recall that the s-process in AGB stars is still uncertain and such a Sr/Ba ratio might also be reproduced this way (26).

Our models offer several predictions for future observations of HMP stars. (1) The metallicity Fe/H of an HMP star is determined by the mass ratios between the ejected Fe M_{Fe} and mixed interstellar H M_{Hmix} , and small M_{Fe} (i.e., small f) is responsible for the small $[\text{Fe}/\text{H}]$. Our spherical explosion models predict a continuous distribution of $[\text{Fe}/\text{H}]$ in metal-poor stars. Thus, if the gap at $[\text{Fe}/\text{H}] \sim -5$ to -4 is real, jet-induced mixing might be responsible for constraining the distribution of the f -value. (2) Assuming that C/H needs to be higher than a certain value in order to form low-mass HMP stars, C/Fe would tend to be larger for smaller Fe/H. (3) The (Na-Mg-Al)/Fe ratios in HMP stars would show a continuous distribution because their variations are the result of variation of E . (4) If the large N/Fe is attributable to rotation and if rotation can contribute to enhance E , N/Fe would show a positive correlation with (Na-Mg-Al)/Fe.

References

1. A. Weiss, T. G. Abel, V. Hill, Eds., *The First Stars* (Springer-Verlag, Berlin, 2000).
2. T. Abel, G. L. Bryan, M. L. Norman, *Science* **295**, 93 (2002).
3. N. Christlieb *et al.*, *Nature* **419**, 904 (2002).
4. A. Frebel *et al.*, *Nature* **434**, 871 (2005).
5. H. Umeda, K. Nomoto, *Nature* **422**, 871 (2003).
6. R. Schneider, A. Ferrara, R. Salvaterra, K. Omukai, V. Bromm, *Nature* **422**, 869 (2003).
7. N. Christlieb *et al.*, *Astrophys. J.* **603**, 708 (2004).
8. M. S. Bessell, N. Christlieb, B. Gustafsson, *Astrophys. J.* **612**, L61 (2004).
9. S. E. Woosley, T. A. Weaver, *Astrophys. J. Suppl. Ser.* **101**, 181 (1995).
10. H. Umeda, K. Nomoto, *Astrophys. J.* **619**, 427 (2005).
11. M. Turatto, *et al.* *Astrophys. J.* **498**, L129 (1998).
12. A. Chieffi, M. Limongi, *Astrophys. J.* **577**, 281 (2002).
13. R. Cayrel *et al.*, *Astron. Astrophys.* **416**, 1117 (2004).
14. H. Umeda, K. Nomoto, T. Nakamura, in *The First Stars*, A. Weiss, T. G. Abel, V. Hill, Eds. (Springer-Verlag, Berlin, 2000), pp. 150-173.
15. A. Heger, N. Langer, S. E. Woosley, *Astrophys. J.* **528**, 368 (2000).

16. T. Suda, M. Aikawa, M. N. Machida, M. Y. Fujimoto, I. Iben, Jr., *Astrophys. J.* **611**, 476 (2004).
17. A. Chieffi, I. Domínguez, M. Limongi, O. Straniero, *Astrophys. J.* **554**, 1159 (2001).
18. L. Siess, M. Livio, J. Lattanzio, *Astrophys. J.* **570**, 329 (2002).
19. H. Umeda, K. Nomoto, *Astrophys. J.* **565**, 385 (2002).
20. A. Heger, S. E. Woosley, *Astrophys. J.* **567**, 532 (2002).
21. W. Aoki *et al.*, *Astrophys. J.* **561**, 346 (2001).
22. S. Lucatello *et al.*, *Astron. J.* **125**, 875 (2003).
23. S. Goriely, N. Mowlavi, *Astron. Astrophys.* **362**, 599 (2000).
24. V. Hill *et al.*, *Astron. Astrophys.* **387**, 560 (2002).
25. C. Sneden *et al.*, *Astrophys. J.* **591**, 936 (2003).
26. L. Siess, S. Goriely, N. Langer, *Astron. Astrophys.* **415**, 1089 (2004).
27. M. Asplund, N. Grevesse, J. Sauval, in *Cosmic abundances as records of stellar evolution and nucleosynthesis*, F. N. Bash, T. G. Barnes, Eds. (Astronomical Society of the Pacific Conf. Ser., San Francisco, 2004), in press (available at <http://arxiv.org/abs/astro-ph/0410214>).

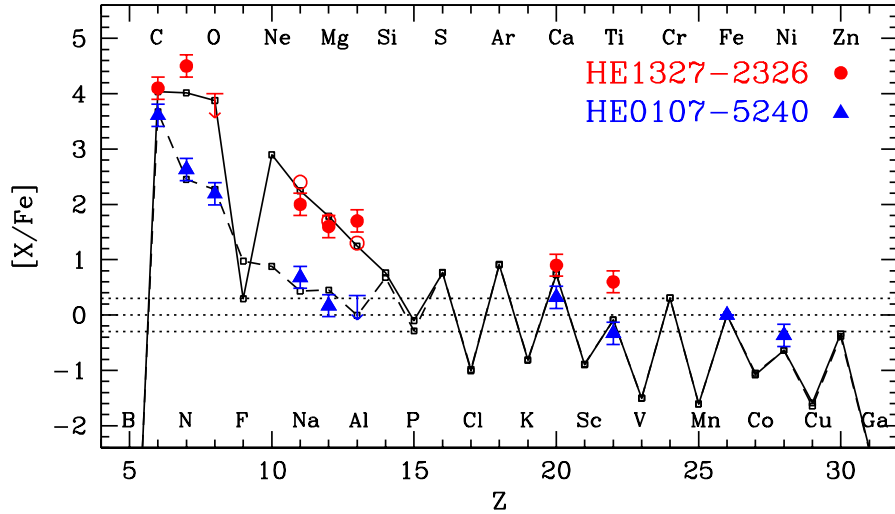


Figure 1: Comparison of elemental abundance ratios observed in HE1327–2326 [filled circles (4)] and HE0107–5240 [filled triangles (7, 8)] with those of our supernova models (small open squares connected by the solid line for HE1327–2326 and by the dashed line for HE0107–5240) as a function of atomic number Z [here the new solar abundances are used (27)]. For Na and Al, the importance of accurate non-local thermodynamic equilibrium (LTE) corrections are demonstrated from the comparison with the LTE values indicated by the open circles. The ejected yields are those from Pop III $25 M_{\odot}$ SN models whose parameters are given in the legend of Figure 2.

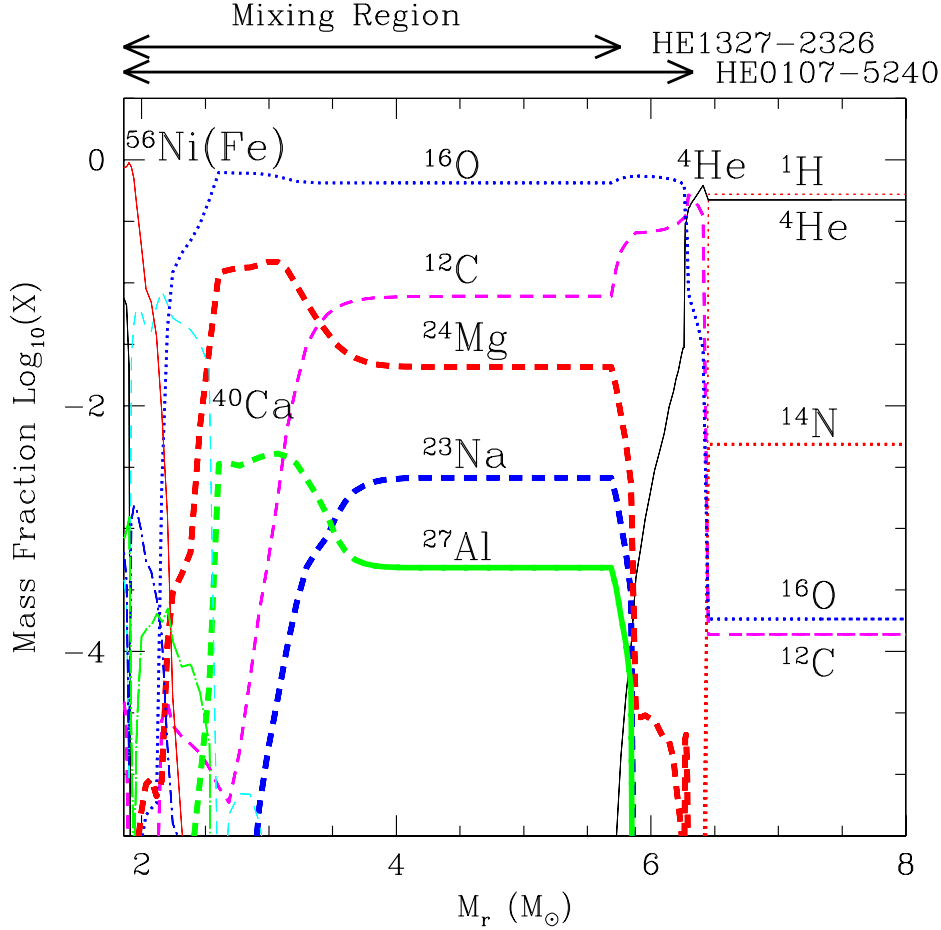


Figure 2: Internal abundance distribution for nuclei (by mass fraction) in the Pop III $25M_{\odot}$ SN model for the explosion energy of $E_{51} = 0.74$ (i.e., for HE1327-2326). The distribution is similar for $E_{51} = 0.71$ (HE0107-5240). The mixing is assumed to take place in the region of $M_r = 1.9 - 5.8M_{\odot}$ for HE1327-2326, and $M_r = 1.9 - 6.3M_{\odot}$ for HE0107-5240. The mass fraction of the ejected materials with respect to the mixed fallback materials is $f = 8.7 \times 10^{-5}$ for HE1327-2326, and $f = 1.2 \times 10^{-4}$ for HE0107-5240. As a result, the ejecta contains $1.0 \times 10^{-5}M_{\odot}$ ^{56}Ni and $0.20 M_{\odot}$ ^{12}C for HE1327-2326, and $1.4 \times 10^{-5}M_{\odot}$ ^{56}Ni and $0.12 M_{\odot}$ ^{12}C for HE0107-5240.

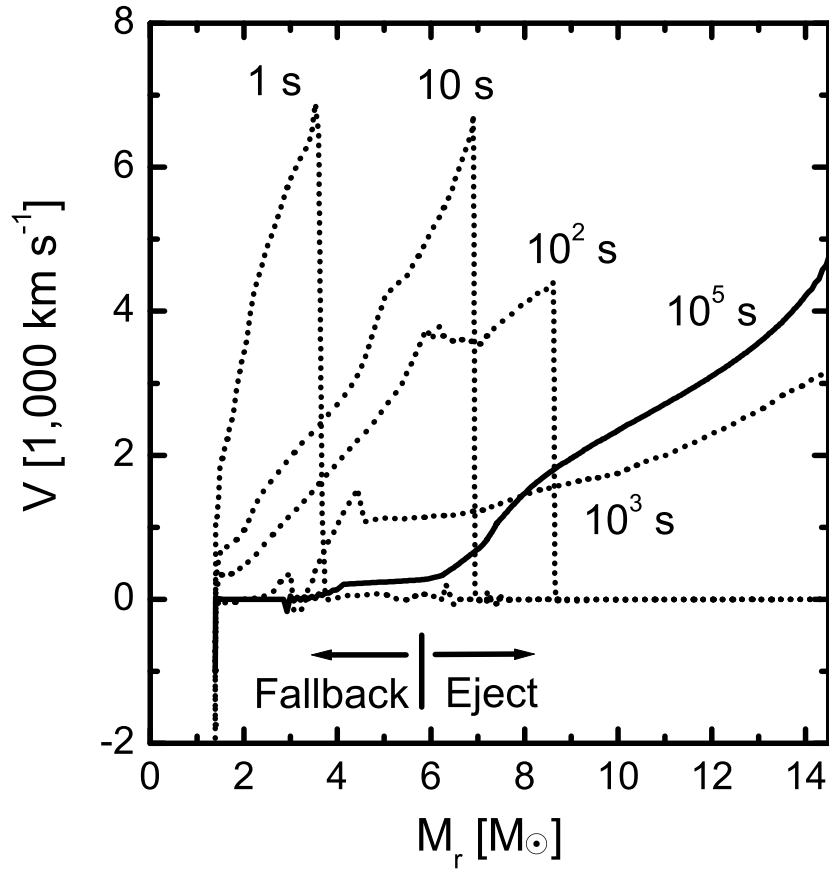


Figure 3: Propagation of the shock wave and the fallback of the model for HE1327–2326. The progenitor is the $25 M_{\odot}$ star. As the shock propagates through the H envelope and breaks out of the surface, the materials in the inner region continue to be decelerated and will eventually fallback onto the central remnant. The mass cut (that divides the materials fallen onto the central remnant and ejected outward) is determined by comparing the velocity and the escape velocity at 10^5 seconds after the explosion.